Education

DYE-SENSITIZED SOLAR CELLS (DSSC): AN APPROACH TO PRACTICE IN UNDERGRADUATE TEACHING

Jeniffer M. Moreira[a,*], Karine C. dos Santos[a], Matheus I. Garcia[a], Raphael Rodrigues[a], Thiago Sequinel[a], Daiane Roman[a] and Cláudio T. de Carvalho[a]

[a]Faculdade de Ciências Exatas e Tecnologias, Universidade Federal da Grande Dourados, 79804-970 Dourados – MS, Brasil

Recebido em 28/04/2023; aceito em 20/10/2023; publicado na web 22/11/2023

The aim of this work was to construct and characterize dye-sensitized solar cells (DSSC) using alternative materials and low-cost equipment. Instead of using the TiO_2 semiconductor, a water-based white paint pigment was employed as a substitute. This pigment, when combined with natural dyes, absorbs visible light and acts as the photoelectrode. Pencil graphite was utilized to create the conductive layer, serving as the positive electrode. Lugol's solution was employed as the electrolyte to establish electrical contact between the two electrodes. These materials were assembled between two glasses with a conductive surface made of tin oxide doped with fluorine (FTO glass). Subsequently, the assembled devices were exposed to three types of lamps: daylight (45 W), LED (15 W), and halogen (105 W), all positioned at the same height as the solar cell. Voltage and current measurements were taken using a simple multimeter. These results enabled the correlation of theoretical concepts related to absorption (dye) and light emission (lamp) ranges, different types of anchoring groups, and the dye-semiconductor anchoring mode. The voltage and current production were found to depend on the type of lighting source. However, it became evident that several factors beyond those mentioned strongly influenced the energy production mode of the solar cell.

Keywords: dye-sensitized solar cell; natural dyes; interactive class.

INTRODUCTION

In the current global scenario, there is a growing concern about the environmental impact generated by the use of finite resources, such as fossil fuels. This concern has ignited a significant demand for new energy sources, especially renewable and clean alternatives. Consequently, governments and private sectors have been increasingly investing in solar energy, which, according to the Renewable Power Generation Costs in 2021 report by the International Renewable Energy Agency (IRENA),[1] is one of the most cost-effective ways to produce electric power. The cost of photovoltaic solar energy generation has plummeted by more than 88% since 2010, making it even more competitive when compared to conventional energy sources.

The process of generating electric power from solar energy is known as the photovoltaic effect. It occurs when photons from sunlight excite particles in a material, creating an electron flow and generating an electric current. In 1839, the French physicist Edmond Becquerel first observed this phenomenon. Later, in 1883, Charles Fritts constructed the first solar cell using a selenium semiconductor and a thin layer of gold. Despite its low electrical conversion efficiency, it garnered significant attention for being the first device capable of generating energy without burning fuels at that time. Silicon became another crucial material in the development of modern photovoltaic cells, discovered through experiments conducted by Russell Ohl in 1941.[2]

Solar cells are classified into generations, which refer to the development and evolution of technologies over time. Currently, the most commonly used solar cells are the first-generation ones, which can be built from monocrystalline or polycrystalline silicon. Monocrystalline silicon cells have a unique crystal structure, resulting in higher energy efficiency, typically ranging from 15 to 24%. On the other hand, polycrystalline silicon cells consist of multiple crystals, resulting in slightly lower efficiencies, usually ranging from 10 to 18%.[3]

*e-mail: jeniffer.moreira010@academico.ufgd.edu.br

Second-generation solar cells are characterized by the use of alternative semiconductor materials, which differ from the crystalline silicon used in the first generation. Examples of such materials include cadmium telluride (CdTe), amorphous silicon (a-Si), and copper indium gallium selenide (CIGS). These cells aim to enhance efficiency and reduce production costs compared to first-generation cells.[4]

The third generation of solar cells encompasses emerging technologies striving for higher efficiency and innovative concepts. This includes organic solar cells, perovskite solar cells, quantum dot solar cells, and dye-sensitized solar cells (DSSC), also known as Grätzel cells, named after their inventor Michael Grätzel, who introduced them in the early 1990s.[5,6] These technologies are in the development and research phase, with the goal of surpassing the limitations of previous generations and delivering significant improvements in terms of efficiency, flexibility, and cost.

An especially remarkable characteristic of DSSCs is their ability to operate efficiently even under low-light conditions, making them a promising solution, especially for low-power applications such as electronic device chargers and standalone systems. DSSCs are particularly well-suited for indoor light harvesting due to their outstanding photovoltage, strong absorption of UV-visible light, and spectral response similar to that emitted by modern indoor lighting systems. This makes them an attractive option for integration into home and building management systems.[7]

Structure and operating principles of DSSCs: the composition of DSSCs, as illustrated in Figure 1, consists of two commercially available conductive glasses, typically FTO (fluorine-doped tin oxide) or ITO (indium-tin oxide), referred to as the anode and cathode. At their interface, a charge mediator is present, usually a liquid solution containing the triiodide/iodide redox pair. The anode, or photoelectrode, is constructed from a semiconductor, usually nanoparticulate titanium oxide (TiO_2 anatase), with an adsorbed dye on its surface. The dye can be composed of organic molecules or metal complexes responsible for absorbing incident photons (hv). These photons excite and inject electrons from the dye into the conduction band of TiO_2 (Figure 1, enlarged detail, and Equations 1 and 2).

Consequently, the dye loses one electron and becomes oxidized (Equation 2). Meanwhile, the cathode, also known as the counter electrode, consists of a thin layer of conductive material (such as graphite, carbon black, or commercial platinum paste, etc.) deposited on the conductive glass. The cathode is responsible for receiving electrons from the anode and transferring them to the electrolyte to regenerate it by reducing triiodide (Equation 3). Simultaneously, the oxidized dye molecule receives electrons from iodide in the electrolyte (Equation 4) to replace the injected electron, thus completing the operational cycle.[8-12]

$$Dye_{(adsorbed)} + h\nu \rightarrow Dye^{*}_{(adsorbed)} \quad (1)$$

$$Dye^{*}_{(adsorbed)} \rightarrow Dye^{+}_{(adsorbed)} + e^{-}_{(injected)} \quad (2)$$

$$I_3^- + 2e^-_{(counter\ electrode)} \rightarrow 3I^- \quad (3)$$

$$2Dye^{+}_{(adsorbed)} + 3I^- \rightarrow Dye_{(adsorbed)} + I_3^- \quad (4)$$

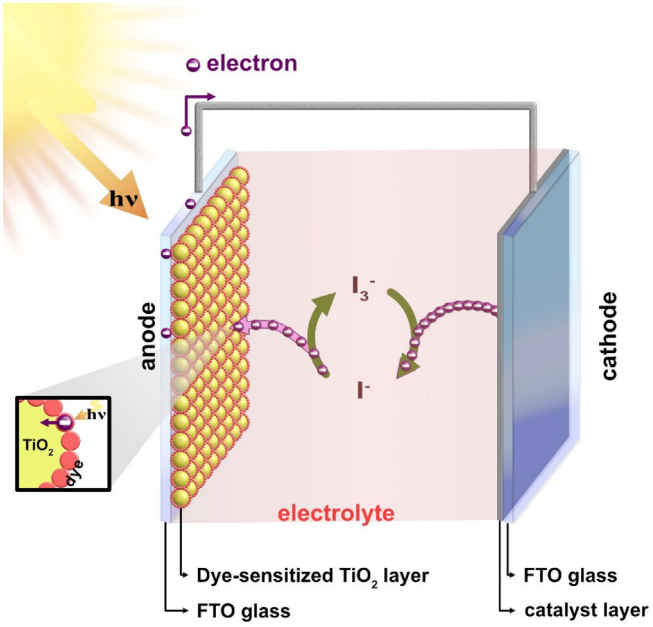

Figure 1. *The image depicts, in a simplified way, the composition and operation of a DSSC-type solar cell. Note that the yellow circles represent TiO_2 nanoparticles, while the red circles depict dye molecules attached to the nanoparticles. In addition to the previously mentioned components, this figure also illustrates sunlight as it illuminates the solar cell*

The quality of DSSCs is highly influenced by the energy levels of the highest occupied molecular orbital (HOMO) and the lowest unoccupied molecular orbital (LUMO) of the dye concerning the conduction band of the semiconductor and the energy levels of the electrolyte. For electron injection, the LUMO must be sufficiently more negative (higher energy) than the conduction band of TiO_2; the energy gap between the two levels is the driving force for electron injection. Similarly, the HOMO must be sufficiently more positive (lower energy) than the redox potential of I^-/I_3^- to effectively accept electrons. The favorable arrangement allows for the efficient transfer of photoexcited electrons from the dye to the TiO_2, facilitating the conversion of light energy into electrical energy in the DSSC system.[13]

This type of solar cell typically achieves efficiency values of approximately 11%, which can vary depending on the components present and the assembly methods employed.[14]

Considering the construction of solar cells using alternative materials as a tool for theoretical-experimental teaching, this work presents an approach to building and discussing the operating cycle of DSSC-type solar cells. In the experiment, a DSSC was developed using natural dyes as photosensitizers and readily available materials and reagents found in commerce. The electric voltage and current produced by the photoelectrochemical systems were monitored using a conventional multimeter. As such, this experiment was designed to convey fundamental concepts related to DSSC cell operations. It is expected that this material can assist in planning low-cost theoretical-experimental classes and serve as an incentive for ongoing adaptations and improvements in the experiment.

EXPERIMENTAL

Materials

FTO conducting glass (resistance < 10 ohm m^{-2}, thickness of 2.2 mm, and transmittance > 82%), blackberry, beetroot, and annatto seeds in powder form; *cis*-bis(isothiocyanato)bis(2,2'-bipyridyl-4,4'-dicarboxylato)ruthenium(II); 5% Lugol solution; water-based white paint pigment; 8B pencil; absolute ethyl alcohol; multimeter; alligator clip connectors; heating plate; tweezers; beaker; filter paper; neutral detergent; distilled water; 3M Magic Tape®; glass rod; Pasteur pipette; binder clip; mortar and pestle; daylight 45 W, halogen 105 W, and LED 15 W lamps.

Preparation of conductive glasses

The DSSC cells were constructed using a glass substrate with a thin FTO film (6.25 cm^2) and an active area of 2.25 cm^2, which were acquired via on-line shopping from China (10 pieces measuring 5 cm × 5 cm can produce up to 40 pieces of approximately 6.25 cm^2). The FTO substrate should be cleaned with neutral detergent, followed by rinsing with distilled water and a final rinse with absolute ethyl alcohol, taking care not to damage the conductive layer on the glass surface.

After cleaning, the conductive glass surface is identified by measuring the electrical resistance using a multimeter, positioning the rotary switch in "Ω", Figure 2a. Once the conductive surface is identified, the anode and cathode constituent materials are deposited.

Anode preparation

Deposition of the semiconductor layer

As an alternative to using pure TiO_2, the semiconductor layer was prepared by initially limiting the active cell area to 2.25 cm^2 using 50 μm thick adhesive tape (3M Magic Tape®). Subsequently, water-based white paint pigment, readily available from hardware stores, was applied to the conductive glass using the doctor blade technique. In this process, a few drops of the material were placed on top of the FTO conductive glass, and a glass rod was then used to evenly spread the material over the surface, creating a thin layer (as depicted in Figure 2b). This method allows for precise control of the cell's active area, ensuring a consistent and defined region for the deposition of the white pigment. After this step, the tape is removed, and the material is heated under a heating plate for approximately 20 min at an average temperature of 300 °C (as shown in Figure 2d). During the heating, the titania layer undergoes a noticeable change, first turning brown/yellow and releasing fumes, and then returning to its original white color. This transformation corresponds to the evaporation and combustion of the non-toxic chemicals present in the paint formulation. Furthermore, the thermal treatment enhances the contact between the TiO_2 particles, resulting in improved electrical connectivity among the oxide particles.[15]

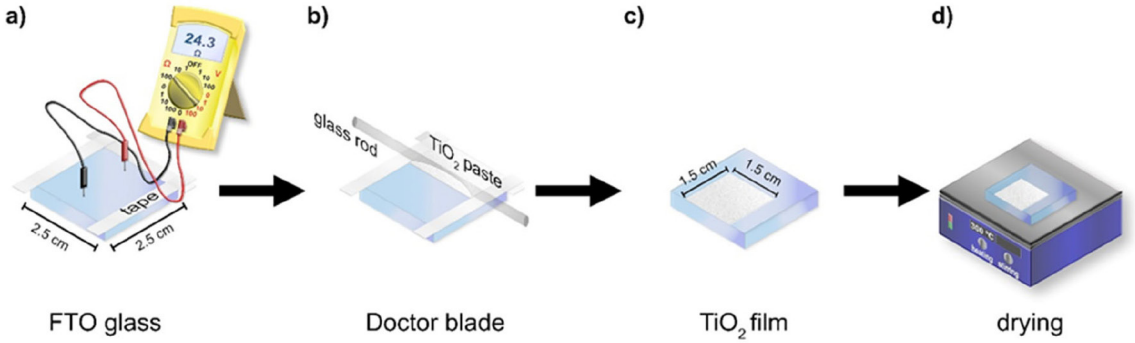

Figure 2. *Image showing the operation sequence used in the doctor blade technique for depositing the semiconductor layer: (a) identification of the conductive surface of the glass and limitation of the active area of the cell with adhesive tape, (b) deposition of water-based white paint pigment, using a glass rod, (c) removal of the adhesive tape and subsequent (d) drying under the heating plate*

Preparation of dye solution

The natural dyes were obtained from blackberries (*Morus nigra*), beetroot (*Beta vulgaris* L.), and annatto seeds (*Bixa orellana* L.). The blackberry dye was obtained by mashing the fruits with a mortar and pestle until obtaining concentrated juice. Alcoholic extraction was required for beetroot and annatto. For beetroot, approximately 50 g of raw beetroot, previously peeled and cut into small pieces, were placed in a beaker with 100 mL of absolute ethanol for 12 h. The annatto extract was obtained from 0.5 g of annatto seed powder and 10 mL of absolute ethanol for the same period. Additionally, a commercial ruthenium(*cis*-bis(isothiocyanato)bis(2,2'-bipyridyl-4,4'-dicarboxylato) ruthenium(II)) dye solution in 0.01 mol L^{-1} of ethanol, known as N3, was also used for comparative purposes, although its use in reproducing this experiment is entirely optional. Following these processes, all solutions were filtered, stored in amber bottles, and kept in the refrigerator until use.

Adsorption of dyes

The glasses with the semiconductor film, after slowly cooling down to room temperature, should be immersed in beakers containing the respective dye solutions and left to rest for approximately 20 h in the dark to ensure maximum adsorption of the dyes on the semiconductor surface. Subsequently, the electrodes were removed from the solution with the help of tweezers and washed with absolute ethanol to remove any excess material that had not adhered. They were then dried on a heating plate for 10 min at 40 °C, forming the anode, also known as the negative electrode or photodetector.

Cathode preparation

The cathode, also referred to as the positive electrode or counter electrode, was prepared using a second piece of FTO with the deposition of a graphite layer as an alternative to the platinum catalytic layer. The graphite layer was obtained by gently rubbing an 8B pencil on the previously tested conductive surface of the glass, using a multimeter. The thin graphite layer serves as a catalyst for the triiodide-to-iodide regeneration reaction. No mask or tape is required for the electrode, and therefore, the entire surface is coated with graphite, as shown in Figure 3.

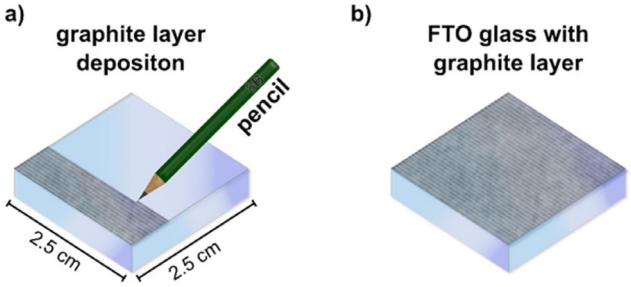

Figure 3. *Image demonstrating the graphite counter electrode manufacturing procedure: (a) rubbing the pencil against the conductive side of the glass, and (b) glass completely coated with graphite*

Closing and inserting the electrolyte

After preparing the electrodes, they are connected together in a "sandwich" configuration, with the two conductive and coated sides facing inward, using binder clips. At the ends of the FTO glass plates, space is reserved for attaching "alligator clips" connectors to establish electrical contact between the positive side (counter electrode) and the negative side (photoelectrode), as shown in Figure 4a. To fill the gap between the electrodes, an electrolytic solution containing iodide/triiodide ions is introduced using a syringe with a needle, a Pasteur

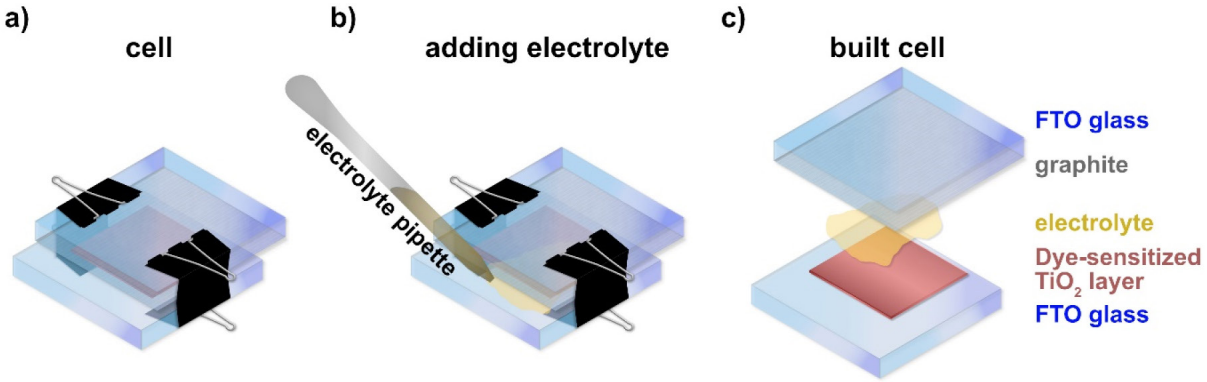

Figure 4. *(a) Cell closure; (b) electrolyte insertion; (c) illustrative image showing cell composition after completion*

pipette, or a dropper. A commonly used option is a 5% Lugol solution (a pharmaceutical product), but a 2% iodine tincture can also be a suitable alternative. Figure 4c provides a detailed illustration of the composition and structure of the assembled cell.

Electric measurements of DSSC cell

To test the operation of the solar cell, voltage and current were measured using a digital multimeter. For these measurements, the test leads, one black and one red, were connected to the "COM" and "VΩmA °F" terminals of the multimeter, respectively. These test leads were then connected to the glass plates containing the anode (black test lead) and cathode (red test lead) of the constructed cell, using "alligator clip" connectors.

First, measure the DSSC voltage with the multimeter set to DCV (direct current voltage) at the 2000 m setting to measure the output in millivolts. Next, change the multimeter setting to DCA (direct current amperage) to measure the current, adjusting the setting to 2000 μ, and measure the current output in microamperes. During the measurements, it may be necessary to replenish the electrolyte due to evaporation. In such cases, add another drop of electrolyte between the glass plates to reactivate the DSSC cell.

In order to facilitate the execution of the experiment within the classroom or laboratory and enable its execution at night without being hindered by weather conditions or sunlight, light bulbs were used. This choice allows for better reproducibility since the emission from the bulbs is constant and uninterrupted. In the experiment, various light sources were employed to expose the cells to different emission spectra. These light sources, including daylight, halogen, and LED lamps, were installed inside a box, measuring 53 × 42 × 45 cm, as depicted in Figure 5. According to information provided by the lamp manufacturers, each emitted 3000, 1785, and 1350 lumens, respectively, determining the luminous flux or the amount of light generated by the lamps to excite the dye at distinct wavelengths. To ensure comparability, the lamps were positioned at a fixed height of 22 cm and centered in the box. Additionally, the base of the box was marked as the designated position for cell analysis, ensuring that all measurements were taken from the same location. This can be observed in the used box shown in Figure 1S of the supplementary material. This control measure ensures a constant amount of light and angle during measurements, allowing for comparisons between different types of photosensitizing dyes to be made.

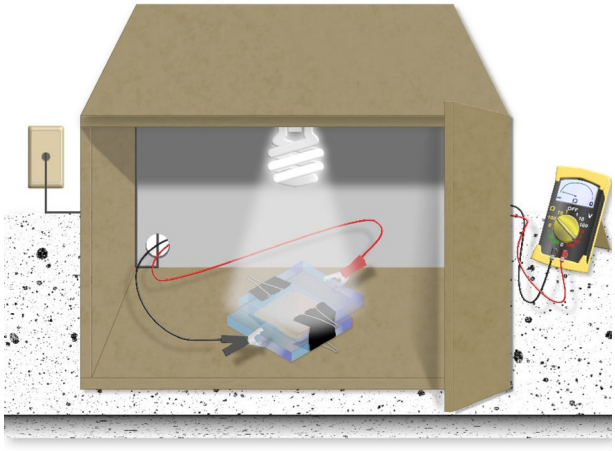

Figure 5. *The box used for irradiating DSSC cells without external light interference*

After completing the experiment, once the cell loses its functionality, it can be disassembled, and the glass plates can be reused for future experiments. Care should be taken while washing them to avoid damaging the conductive layer. The graphite-coated glass should only be used for assembling a new counter electrode, while the white dye-coated glass can be reused as a new photoelectrode.

RESULTS AND DISCUSSION

The efficiency of a DSSC cell is inherently linked to the dye/photosensitizer, as it is responsible for the cell's ability to absorb electromagnetic radiation in the visible region. This is because pure titanium dioxide (TiO_2) exhibits an absorption band in the ultraviolet region and a limited response in the visible region. Sensitizing TiO_2 with a photosensitizer dye becomes essential to broaden its response in the visible spectrum, allowing for greater absorption of light and, consequently, improving the efficiency of solar energy conversion to electricity. Figure 6 displays the absorption spectra in the UV-Vis region of natural dyes extracted from blackberries, beetroot, and annatto seeds, as well as the commercial N3 dye.[16]

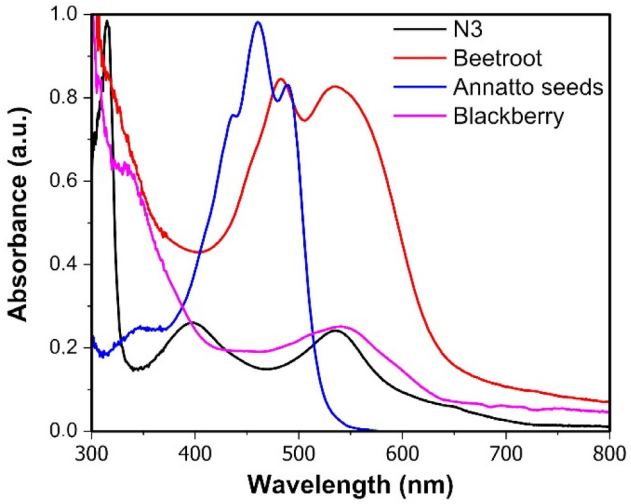

Figure 6. *UV-Vis absorption spectra of the dyes obtained through ethanolic extract*

Natural photosensitizers have a more diverse chemical composition than the ruthenium complex, containing different classes of chemicals, mainly anthocyanins, betalains, and carotenoids, with π-π* and n-π* electronic transitions responsible for absorbing visible light. The annatto seed dye has maximum absorption peaks around 460 nm with a band between 400 and 489 nm. This extract consists of a mixture of carotenoids, with approximately 80% bixin and 20% norbixin.[17] Beetroot dye has absorption peaks at longer wavelengths in the 540 nm region, attributed to the presence of purple-colored betacyanin and an additional peak around 480 nm corresponding to betaxanthin, a yellow betalain.[12,18] Blackberry dye, at wavelengths similar to beetroot, exhibits a maximum absorption peak at 543 nm in the visible region, indicating the predominant presence of cyanidin 3-glucoside, a purple anthocyanin.[19]

Regarding molecular structure, aliphatic and unsaturated carotenoids are capable of absorbing radiation of higher energy (shorter wavelengths) compared to other cyclic and aromatic compounds. From the spectra shown in Figure 6, it is evident that the absorption of carotenoids does not exceed 550 nm.[12,17]

The synthetic dye N3, unlike the others, is a ruthenium(II) metal complex and exhibits intense absorption with a maximum at 316 nm and two broad medium-intensity peaks at 399 and 545 nm. According to literature data, the charge transfer (CT) in this system occurs from the metal to the ligand (ML), which is referred to as metal-ligand

charge transfer (MLCT). In summary, it can be stated that MLCT occurs due to the excitation of electrons from the ground state to the excited state of the ligands (π* orbital) via the bipyridine ring. Figures 7a-7f depict the main chemical structures of the natural dyes and N3, emphasizing the flow of electrons through the anchoring groups of each dye molecule to TiO_2.[20]

In addition to their role in absorbing energy in the visible spectrum, dye electrons must be injected into the conduction band of the TiO_2 semiconductor. The interaction between the dye and TiO_2 can occur through various mechanisms, including electrostatic interaction, hydrogen bonding, hydrophobic interaction, Van der Waals forces, or physical confinement. However, what primarily ensures a strong coupling and, consequently, better electron flow are the covalent bonds formed between the functional groups of the dye (anchoring groups) and the surface atoms of TiO_2. Various chemical functional groups are capable of efficiently bonding to TiO_2. The best anchoring groups are phosphonic acids, followed by carboxylic acids and their derivatives, such as acid chlorides, amides, esters, or carboxylate salts and sulfonic groups, cyanoacrylates, pyridinic, hydroxyl, among others.[16,21-23]

In the chemical structure of the photosensitizers used, Figure 7, the main anchorage group for the annatto, beetroot, and N3 dyes is the carboxylic one. This group anchor to the oxide surface in different ways: monodentate (Figure 7g), bidentate chelate (Figure 7h), or bridge (Figure 7i); the last two forms have two donor atoms. Studies have shown that the form of direct anchoring interferes with the efficiency of electron injection, so bidentate forms are preferable. This form of anchoring provides higher stability compared to the monodentate form due to bonding force, reducing the distance of the anchoring group from the semiconductor surface and, therefore, improving the efficiency of electron injection into the TiO_2 conduction band.[16,24]

Anchoring in the monodentate mode can be associated with betacyanin (Figure 7a) and cyanidin (Figure 7e), which are the only compounds that contain hydroxyl groups in their structure. Moreover, the structure of cyanidin features hydroxyl groups at positions 1 and 2 of the benzene ring, known as catechol. These groups facilitate anchoring to the surface of TiO_2 through a bidentate mononuclear chelate mode (Figure 7k) or even through the dinuclear bridging form (Figure 7l), resulting in improved electron flow within the device.[22]

The photosensitizers (dyes) can be categorized into two types, I and II, based on their electron injection mechanism into the semiconductor oxide. The more common type I involves carboxyl and hydroxyl groups, where electron injection occurs in two steps. First, photoexcitation occurs where electrons transition from the ground state (HOMO) to the excited state (LUMO). Subsequently, these electrons are injected into the TiO_2 conduction band. In this case, the anchoring groups act as electron acceptors due to their strong electron-withdrawing capability and the increased electron density surrounding their structure, facilitating their subsequent injection into

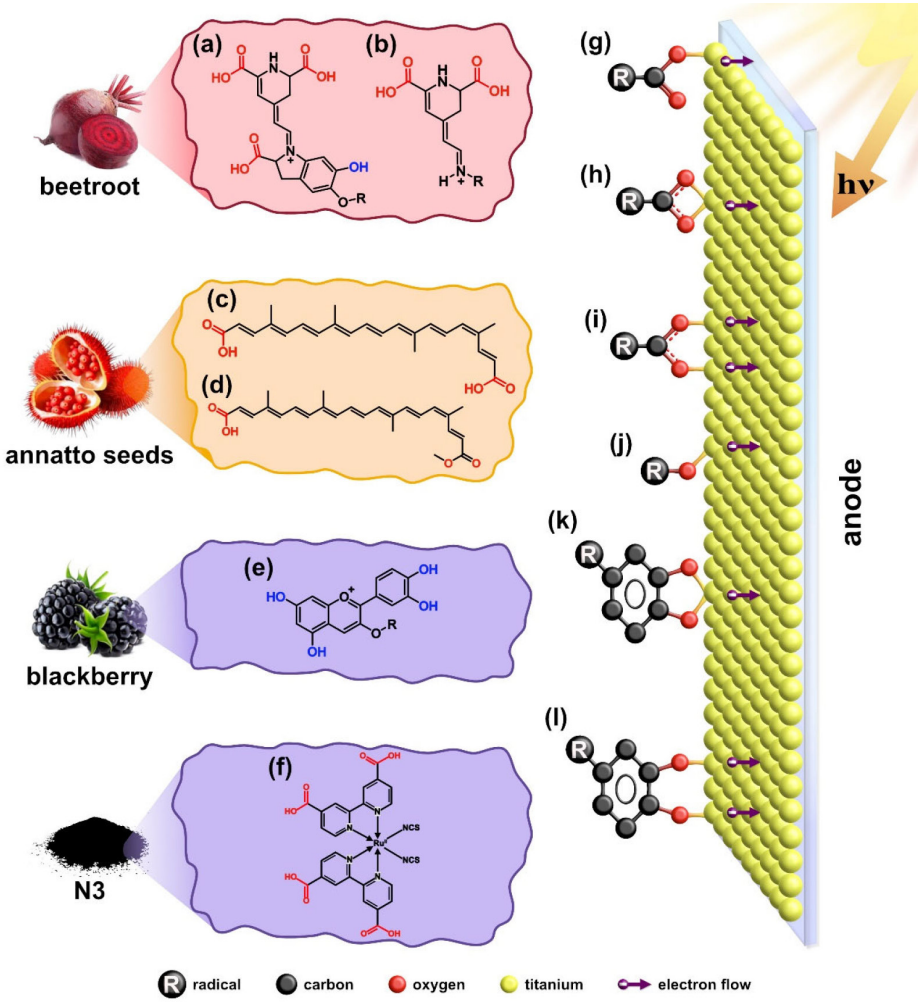

Figure 7. *Main chemical compounds present in the dyes obtained from beetroot: (a) betacyanin and (b) betaxanthin; annatto seeds: (c) norbixin and (d) bixin; blackberry: (e) cyanidin; (f) commercial dye N3 and anchoring mode on the surface of the TiO_2 semiconductor by the carboxylic group: (g) monodentate ester; (h) bidentate chelate; (i) bidentate bridge, hydroxyl; (j) monodentate and catechol; (k) bidentate mononuclear chelate; (l) bidentate dinuclear bridging link*

TiO_2. Type II dyes, such as those with catechol groups (two hydroxyls at positions 1 and 2 of the ring) found in the cyanidin compound, promotes charge transfer directly from the highest occupied molecular orbital (HOMO) of the dye to the TiO_2 conduction band, constituting a single-step electron injection process characterized by a lower electron-withdrawing ability compared to carboxylic groups.[16,22,24]

The N3 dye was employed for comparative purposes with natural dye data, as it is a well-known and extensively studied photosensitizer for DSSC cell assembly. The conversion efficiency of the N3 dye arises from the spatial separation of the LUMO donor orbital, which is close to the TiO_2 conduction band, resulting in a much faster injection. Additionally, it should be noted that the presence of four carboxylate groups provides a strong binding/anchor to the TiO_2 surface, classifying it as a type I dye, while the isothiocyanate (NCS) groups contribute to increased absorption in the visible region.[18]

The process of photoexcitation of the described dyes can be induced by various light sources. Natural sources, such as sunlight, have a broad emission profile covering the ultraviolet region (300-400 nm), visible region (400-700 nm), and near-infrared region (700-2500 nm), with 6, 45, and 49% of the light, respectively. Alternatively, artificial light sources, such as different types of lamps, can be used, providing continuous illumination regardless of the time of day and under various weather conditions. However, it is essential to acknowledge that each lamp emits light within a specific range of wavelengths and intensity, as demonstrated in Figures 2Sa-2Sc.[7]

In the spectrum comparison, the daylight lamp closely resembles solar light on Earth, covering a wide spectral range from UV to infrared, with a maximum emission around 450 nm. The halogen lamp emits radiation starting at approximately 300 nm, with a maximum emission around 590 nm in the visible region. It also emits a small amount of ultraviolet light and a significant amount of infrared light. On the other hand, the LED does not emit ultraviolet or infrared radiation; it has maximum emission peaks at 445 nm (sharp) and another broad peak at 558 nm in the visible range. These radiation emissions at different wavelengths and intensities directly influence how the photosensitizer material (dye) will function in the DSSC-type cell.[25-27]

In this study, the same parameters were used to measure all DSSC devices assembled with different dyes, such as distance from the light source, active area of cells, among others. Figure 8 shows the results of the experiment involving four dye-sensitized DSSCs, which were illuminated with three different light sources. Before delving into the theoretical exploration of the results, it is crucial to clarify two key points regarding the voltage and current produced in a solar cell. Firstly, the voltage generated by a solar cell depends on factors such as light intensity, the effective illuminated area of the cell, and the electrical characteristics of the semiconductor material. Secondly, the current generated by a solar cell is the electric current that flows when charge carriers (electrons and holes) move through the external circuit in response to the electric field created within the cell. This current is directly proportional to the incident light and the cell's efficiency in converting light into electricity. It is important to note that this experiment was not designed to assess the efficiency of the solar cell, as such an evaluation could make the experiment costly and impractical for typical teaching laboratories. Nevertheless, we can briefly summarize cell efficiency as its capacity to convert sunlight energy into usable electricity. Typically expressed as a percentage, efficiency represents the ratio between the electrical power generated by the solar cell and the power of incident sunlight. Higher efficiency indicates a more effective conversion of sunlight into electricity.

Returning to the data presented in Figure 8, we conducted current and voltage measurements using a simple multimeter, which can operate in ammeter or voltmeter modes to measure open-circuit voltage (Voc) (Figure 8a) and short-circuit current (Isc) (Figure 8b). In this dataset, we observe that the annatto seed dye efficiently absorbs light in the visible range between 400 and 550 nm (Figure 6). An important characteristic of the compounds used as photosensitizer materials, responsible for light absorption, is their extended conjugated systems. These systems consist of carbon atoms covalently bonded through alternating single and double bonds. Additionally, the molecules within this extract possess anchoring groups (carboxylic) that serve as effective electron flow directors for the TiO_2 semiconductor. Regarding the light sources, Figure 2S in the supplementary material clearly shows the regions of highest emission for the lamps. Daylight and LED lamps emit radiation at wavelengths with higher intensity within the same dye absorption range (400-550 nm). In contrast, the halogen lamp exhibits greater emission above 500 nm. By correlating this data, it is possible to suggest that the radiation emitted by the LED lamp enhances electron flow in the system. Conversely, the emission from the daylight lamp creates a larger charge difference between the cell poles due to electron movement and gaps, resulting in a greater potential difference.[26,27]

Another example with a somewhat similar behavior is the response observed in the case of blackberry and N3 dyes. Both of these dyes absorb light in the visible region, and their absorption bands practically overlap, with λmax around 550 nm. This characteristic aligns them well with the emission range of the daylight lamp. However, it is important to note that the efficiency of the DSSC cell depends on multiple factors, as previously mentioned. These factors

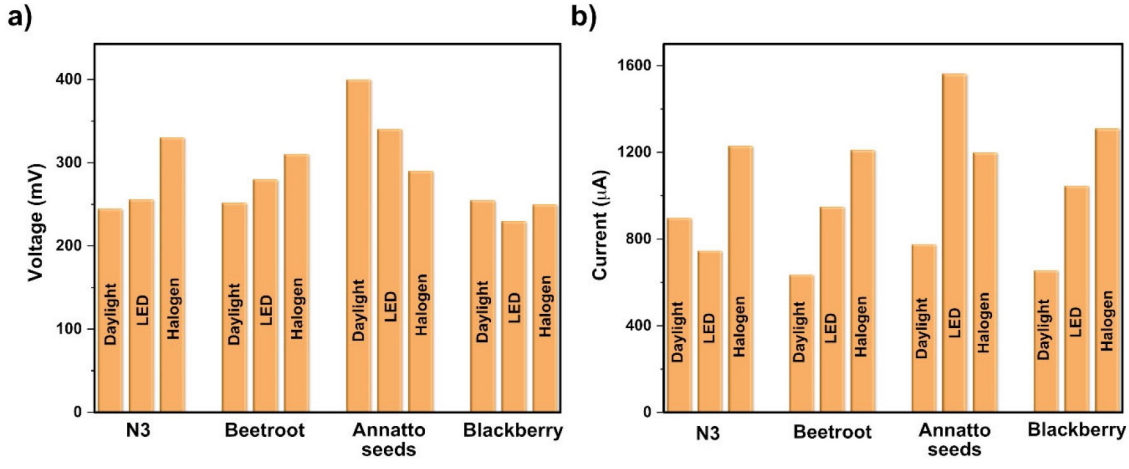

Figure 8. *(a) Voltage and (b) current results obtained for photovoltaic devices built with different photosensitizers/dyes and excitation sources*

include how the dye molecules are anchored to the semiconductor surface and the energy levels of the excited state of each dye. Therefore, the correlations observed cannot solely be attributed to the emission (lamp) and absorption (dye) spectra.[26] In addition to these considerations, it is essential to emphasize that this experiment was designed for classroom environments using cost-effective alternative materials. To ensure reproducibility of the tested device, it's important to acknowledge that the system is open, which can pose challenges such as evaporation and electrolyte replacement, dye degradation, and other complex issues like resistance and charge recombination, among others. Analyzing and addressing these challenges can lead to engaging discussions in academia regarding strategies for improving the electron transfer process. In more advanced analyses, it may involve constructing low-cost electronic devices for plotting an IV curve (current *versus* voltage) and evaluating the cell efficiency within an academic environment or even studying these parameters using a commercial device.[12,13]

CONCLUSION

The use of alternative and cost-effective materials in the construction of DSSCs, such as white paint, graphite pencil, Lugol's solution, and natural dyes extracted from annatto, beet, and blackberry seeds, offers the advantage of an accessible approach to renewable technologies. Traditionally, DSSCs were assembled using expensive ruthenium(II) complexes, which are harder to obtain. To use ruthenium as a dye, it needs to be combined with an organic ligand that possesses specific characteristics. On the other hand, the use of alternative materials, like natural dyes demonstrated in this study, simplifies the conduction of experiments in any academic setting, requiring minimal resources. We believe that this experiment, along with other materials described in the literature, can serve as a starting point for exploring the operation and limitations of photovoltaic devices. It also encourages their construction and electrical characterization in teaching laboratories. However, the energy generation process in a cell is complex and depends on factors such as light intensity, cell area, temperature, and incidence angle, among many others. Therefore, this study did not aim to evaluate all of these parameters but rather focused on observing the behavior of the cells when illuminated with different light sources of varying power, while measuring the voltage (open-current voltage) and current (short-circuit current) at the device's output. In conclusion, active teaching methodologies, such as hands-on experiments, are becoming increasingly important in higher education as they engage and inspire students. By introducing students to technologies like DSSCs, educators can foster greater interest in renewable energy and sustainable solutions to global challenges.

SUPPLEMENTARY MATERIAL

Figures 1S and 2S are available in the supplementary material at http://quimicanova.sbq.org.br in pdf format, with free access.

ACKNOWLEDGMENT

The authors thank Brazilian Foundations CNPq, FUNDECT, CAPES, and Finep for financial support, and professional N. M. de Carvalho for english reviewing.

REFERENCES

1. International Renewable Energy Agency (IRENA); *Renewable Power Generation Costs in 2021*, Abu Dhabi, United Arab Emirates, 2022. [Link] accessed in November 2023
2. Vitoreti, A. B. F.; Vaz, R.; Pena, A. D. L.; Raphael, E.; Ferrari, J. L.; Schiavon, M. A.; *Rev. Virtual Quim.* **2017**, *9*, 1481. [Crossref]
3. Pastuszak, J.; Wegierek, P.; *Materials* **2022**, *15*, 5542. [Crossref]
4. Ramanujam, J.; Bishop, D. M.; Todorov, T. K.; Gunawan, O.; Rath, J.; Nekovei, R.; Artegiani, E.; Romeo, A.; *Prog. Mater. Sci.* **2020**, *110*, 100619. [Crossref]
5. Mai, C. L.; Huang, W. K.; Lu, H. P.; Lee, C. W.; Chiu, C. L.; Liang, Y. R.; Diau, E. W. G.; Yeh, C. Y.; *Chem. Commun.* **2010**, *46*, 809. [Crossref]
6. Machado, C. T.; Miranda, F. S.; *Rev. Virtual Quim.* **2015**, *7*, 126. [Crossref]
7. Kim, S.; Jahandar, M.; Jeong, J. H.; Lim, D. C.; *Current Alternative Energy* **2019**, *2*, 3. [Crossref]
8. Richhariya, G.; Kumar, A.; Tekasakul, P.; Gupta, B.; *Renewable Sustainable Energy Rev.* **2017**, *69*, 705. [Crossref]
9. Khan, J.; Arsalan, M. H.; *Renewable Sustainable Energy Rev.* **2016**, *55*, 414. [Crossref]
10. Vougioukalakis, G. C.; Philippopoulos, A. I.; Stergiopoulos, T.; Falaras, P.; *Coord. Chem. Rev.* **2010**, *255*, 2602. [Crossref]
11. Cavallo, C.; Pascasio, F. D.; Latini, A.; Bonomo, M.; Dini D.; *J. Nanomater.* **2017**, *2017*, 31. [Crossref]
12. Sonai, G. G.; Melo, M. A.; Nunes, J. H. B.; Megiatto, J. D.; Nogueira, A. F.; *Quim. Nova* **2015**, *38*, 1357. [Crossref]
13. Sharma, K.; Sharma, V.; Sharma, S. S.; *Nanoscale Res. Lett*. **2018**, *13*, 381. [Crossref]
14. Chiba, Y.; Islam, A.; Watanabe, Y.; Komiya, R.; Koide, N.; Han, L.Y.; *Jpn. J. Appl. Phys.* **2006**, *45*, L638. [Crossref]
15. Martineau, D.; *Dye Solar Cells for Real: The Assembly Guide for Making Your Own Solar Cells*, Switzerland, 2012. [Link] accessed in November 2023
16. Hagfeldt, A.; Boschloo, G.; Sun, L.; Kloo, L.; Pettersson, H.; *Chem. Rev.* **2010**, *110*, 6595. [Crossref]
17. Gómez-Ortíz, N. M.; Vázquez-Maldonado, I. A.; Pérez-Espadas, A. R.; Mena-Rejón, G. J.; Azamar-Barrios, J. A.; Oskam, G.; *Sol. Energy Mater. Sol. Cells* **2010**, *94*, 40. [Crossref]
18. Zhang, D.; Lanier, S. M.; Downing, J. A.; Avent, J. L.; Lum, J.; Mchale, J. L.; *J. Photochem. Photobiol., A* **2008**, *195*, 72. [Crossref]
19. Senthil, T. S.; Muthukumarasamy, N.; Velauthapillai, D.; Agilan, S.; Thambidurai, M.; Balasundaraprabhu, R.; *Renewable Energy* **2011**, *36*, 2484. [Crossref]
20. Persson, P.; Lundqvist, M. J.; *J. Phys. Chem. B* **2005**, *109*, 11918. [Crossref]
21. Marwa, B. M.; Bruno, S.; Mongi, B.; Tran Van, F.; Abdelmottaleb, B. L.; *Sol. Energy* **2016**, *135*, 177. [Crossref]
22. Zhang, L.; Cole, J. M.; *ACS Appl. Mater. Interfaces* **2015**, *7*, 3427. [Crossref]
23. Hug, H.; Bader, M.; Mair, P.; Glatzel, P.; *Appl. Energy* **2014**, *115*, 216. [Crossref]
24. Ooyama, Y.; Yamaii, K.; Ohshita, J.; *Mater. Chem. Front.* **2017**, *11*, 2243. [Crossref]
25. Ladomenou, K.; Kitsopoulos, T. N.; Sharma, G. D.; Coutsolelos, A. G.; *RSC Adv.* **2014**, *4*, 21379. [Crossref]
26. Junger, I. J.; Werner, D.; Hellkamp, E. S.; Ehrmann, A.; *Optik* **2019**, *117*, 8. [Crossref]
27. Western Caroline University, https://agora.cs.wcu.edu/~huffman/lectures/uvvis.html, accessed in November 2023